

# Implementing topological quantum manipulation with superconducting circuits

Zheng-Yuan Xue,<sup>1</sup> Shi-Liang Zhu,<sup>2,1</sup> J. Q. You,<sup>3</sup> and Z. D. Wang<sup>1</sup>

<sup>1</sup>*Department of Physics and Center of Theoretical and Computational Physics,  
The University of Hong Kong, Pokfulam Road, Hong Kong, China*

<sup>2</sup>*Laboratory of Quantum Information Technology, ICMP and SPTE,  
South China Normal University, Guangzhou 510006, China*

<sup>3</sup>*Department of Physics and Surface Physics Laboratory (National Key Laboratory),  
Fudan University, Shanghai 200433, China*

(Dated: November 3, 2018)

A two-component fermion model with conventional two-body interactions was recently shown to have anyonic excitations. We here propose a scheme to physically implement this model by transforming each chain of two two-component fermions to the two capacitively coupled chains of superconducting devices. In particular, we elaborate how to achieve the wanted operations to create and manipulate the topological quantum states, providing an experimentally feasible scenario to access the topological memory and to build the anyonic interferometry.

PACS numbers: 03.67.Lx, 42.50.Dv, 85.25.Cp

Topological ordered states emerge as a new kind of states of quantum matter beyond the description of conventional Landau's theory [1], whose excitations are anyons satisfying fractional statistics. A paradigmatic system for the existence of anyons is a kind of so-called fractional quantum Hall states [2]. Alternatively, artificial spin lattice models are also promising for observing these exotic excitations [1, 3, 4]. Kitaev models [3, 4] are most famous for demonstrating anyonic interferometry and braiding operations for topological quantum computation.

Since anyons have not been directly observed experimentally, a focus at present is to experimentally demonstrate the topological nature of these states. Abelian anyons maybe relatively easy to achieve and to manipulate in comparison with the nonabelian ones, thus it is of current interest to explore them both theoretically and experimentally. Kitaev constructed an artificial spin model [3], i.e., the toric code model, which supports the abelian anyon. But the wanted four-body interactions are notoriously hard to generate experimentally in a controllable fashion. Alternatively, it was proposed [5] to generate dynamically the ground state and the excitations of the model Hamiltonian, instead of direct ground-state cooling, to simulate the anyonic interferometry. On the other hand, implementation of another Kitaev's honeycomb model [4] was also suggested in the context of ultracold atoms [6], polar molecules [7], and superconducting circuits [8]. The honeycomb model [4] is an anisotropic spin model with three types of nearest-neighbor two-body interactions, which support both abelian and nonabelian anyons. It was shown [4] that the toric code model can be obtained from the limiting case of the honeycomb model. Using this map, preliminary operations for topological quantum memory and computation were also addressed [9, 10, 11, 12]. Nevertheless, in this case, anyons are created by the fourth-order perturbation treatment, which would blur the extracted anyonic information [12]. In addition, this map is good but not exact, so that one may get both anyonic and fermionic excitations. Therefore, new methods for implementing the model and manipulating the relevant topological states are still desirably awaited.

Recently, a two-component fermion model [13] with conventional two-body interactions was shown to have anyonic excitations, which obey the same fusion rules as those of the toric code model and are mutual semions. This model is promising because it provides an example for abelian anyons, which can be directly implemented. In this Rapid Communication, we propose to physically implement this model with appropriately designed superconducting circuits. In particular, we elaborate how to achieve the wanted operations that create and manipulate the topological states as well as anyons with the cavity-assisted interactions using an external magnetic drive, providing an experimentally feasible scenario to access the topological memory and to build the anyonic interferometry.

The Hamiltonian for the two-component fermion model in a two-dimensional square lattice, as shown in Fig. 1(a), is [13]

$$\begin{aligned}
 H_{f1} = & -J_q \sum_{\langle i,j \rangle} (2n_{\uparrow,i} - 1)(2n_{\uparrow,j} - 1) \\
 & -J_p \sum_{\langle i,j \rangle} (2n_{\downarrow,i} - 1)(2n_{\downarrow,j} - 1) \\
 & +U \sum_i (2n_{\uparrow,i} - 1)(2n_{\downarrow,i} - 1), \quad (1)
 \end{aligned}$$

where  $n_{s,i} = c_{s,i}^\dagger c_{s,i}$ ,  $c_{s,i}$  are annihilation operators of spin- $s$  fermions, and  $\langle i, j \rangle$  mean the nearest neighbors along the horizontal diagonals of squares. The ground states of this Hamiltonian are highly degenerated, i.e., every individual chain is ferromagnetic. As shown in Ref. [13], the low-lying excitations are deconfined mutual semions under the open boundary condition.

To show the nature of the low-lying excitations, we map the square lattice to the honeycomb lattice, as shown in Fig. 1(b), by extending each lattice site in the square lattice to be a vertical link of Majorana fermions [see Fig. 1(c)] defined by  $\psi_{i_b} = -i(c_{\uparrow,i} - c_{\uparrow,i}^\dagger)$ ,  $\psi_{i_w} = c_{\uparrow,i} + c_{\uparrow,i}^\dagger$ ;  $\chi_{i_b} = -i(c_{\downarrow,i} - c_{\downarrow,i}^\dagger)$ , and  $\chi_{i_w} = c_{\downarrow,i} + c_{\downarrow,i}^\dagger$ . These "real" fermion operators obey  $\psi_{i_s}^2 = \chi_{i_s}^2 = 1$ . Otherwise, they are anticommutative. In

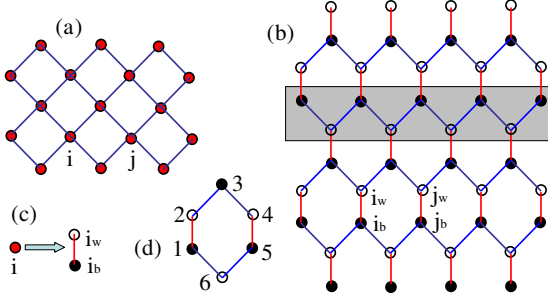


FIG. 1: (Color online) A map from a square lattice to a honeycomb lattice by extending each square lattice site to be a vertical link. (a) The square lattice, where  $\langle i, j \rangle$  denotes the nearest neighbors along the horizontal diagonal direction. (b) The honeycomb lattice, where  $i_{b,w}$  label the black and white sublattices. The indicated zig-zag chain is one of the lines for the Jordan-Wigner transformation. (c) Each square lattice site being extended as a vertical link of Majorana fermions with  $i_w$  ( $i_b$ ) labels the white (black) sublattice and  $i_w$  on the top of  $i_b$ . (d) Site-labels within a plaquette.

this Majorana fermion representation, the Hamiltonian (1) is mapped to

$$H_{f2} = -J_q \sum_{\langle ij \rangle} W_{ij} - J_p \sum_{\langle ij \rangle} \tilde{W}_{ij} + U \sum_i Q_i \tilde{Q}_i, \quad (2)$$

where  $W_{i,j} = Q_i Q_j$  with  $Q_i = i\psi_{i_w}\psi_{i_b}$  and  $\tilde{W}_{ij} = \tilde{Q}_i \tilde{Q}_j$  with  $\tilde{Q}_i = i\chi_{i_w}\chi_{i_b}$ . Since there is no coupling between the chains, the present model may be transferred to a spin model

$$H_{f3} = -J_q \sum_P W_P - J_p \sum_P \tilde{W}_P - U \sum_i S_{i_b}^z S_{i_w}^z, \quad (3)$$

by using Jordan-Wigner transformation [14]:  $\psi_{j_w} = S_{j_w}^y \prod_{j'_s < j_w} S_{j'_s}^z$ ,  $\psi_{j_b} = S_{j_b}^x \prod_{j'_s < j_b} S_{j'_s}^z$ ,  $\chi_{j_w} = S_{j_w}^x \prod_{j'_s < j_w} S_{j'_s}^z$ , and  $\chi_{j_b} = S_{j_b}^y \prod_{j'_s < j_b} S_{j'_s}^z$ , where  $S^{x,y,z}$  are the corresponding Pauli matrices for the defined Majorana fermions,  $W_P = S_1^x S_2^y S_3^z S_4^x S_5^y S_6^z$  and  $\tilde{W}_P = S_1^x S_2^y S_3^z S_4^x S_5^y S_6^z$  with the site labels within a plaquette depicted in Fig. 1(d). The order of the sites is defined as follows:  $j_s > j_t$  if the zigzag line [one of such lines is indicated in Fig. 1(b)] including  $j_s$  is higher than that of  $j_t$ , or if  $j_s$  is on the right hand of  $j_t$  when they are in the same line. It is straightforward to check  $[W_P, \tilde{W}_{P'}] = 0$  for every plaquette, and all of them also commute with the third term. In this spin model, the ground state can be written as

$$|G\rangle = \prod_P (1 + W_P)(1 + \tilde{W}_P)|\phi\rangle, \quad (4)$$

where  $|\phi\rangle = |1 \cdots 1\rangle$  is a reference state and each "1" means the eigenvalue of  $S_{j_b(w)}^z$  being 1. Similar to the Kitaev's honeycomb model [4], all excitations here may be labelled by two quantum numbers  $W_P$  and  $\tilde{W}_P$ . The low energy excitations fall into two closed subsets, each can be graded by a  $Z_2 \times Z_2$  group. The fusion rules of these excitations are equivalent to the excitations in the toric code model [3], and different graded vortices are mutual abelian semions [15].

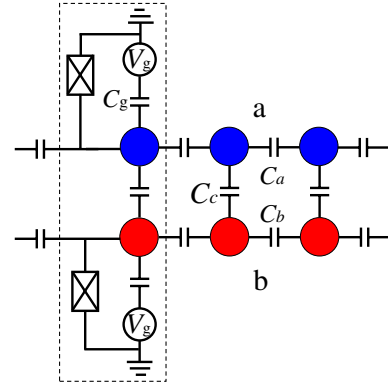


FIG. 2: (Color online) A schematic circuit of two chains of capacitively coupled superconducting devices, labeled by  $a$  and  $b$ , to implement a chain of two-component fermions. Here only the first device of the two chains is explicitly shown, while others are simply denoted as the filled circles with different colors (shades) for different chains.

We now proceed to implement the model with capacitively coupled superconducting devices, i.e., the Cooper pair box. The key idea is to use two chains of capacitively coupled superconducting devices, as shown in Fig. 2, to implement a chain of two-component fermions. A building block of our implementation, as shown in the rectangle of Fig. 2, is the two capacitively coupled superconducting devices. A typical design of a Cooper pair box consists of a small superconducting island with  $n$  excess Cooper pair charges connected by a Josephson junction with coupling energy  $E_J$  and capacitance  $C_J$ . A control gate voltage  $V_g$  is applied via a gate capacitor  $C_g$ . To quantize the circuit equation, we first introduce the Hamiltonian and then convert the classical momentum variable to the momentum operator. Then the Hamiltonian reads

$$H_{q1} = \sum_\eta \left[ \frac{\alpha C_t^\eta}{2} (\dot{\varphi}^\eta)^2 - E_J^\eta \cos \varphi^\eta \right] - \alpha C \dot{\varphi}^a \dot{\varphi}^b, \quad (5)$$

where  $\varphi^\eta$  is the gauge phase drop across the corresponding junction,  $C_t^\eta = C_0^\eta + C_c$  with  $C_0^\eta = C_g^\eta + C_J^\eta$ ,  $\alpha = (\hbar/2e)^2$ , and the induced charge  $n_g^\eta = C_g^\eta V_g^\eta / 2e$ . At temperatures much lower than the single-pair charging energy, i.e.,  $k_B T \ll E_c^\eta = e^2 / (2C_0^\eta)$ , and restricting the gate charge to the range of  $n_g \in [0, 1]$ , only a pair of adjacent charge states  $\{|0\rangle, |1\rangle\}$  on the island are relevant. The Hamiltonian (5) is then reduced to [16]

$$H_{q2} = -\frac{1}{2} \sum_\eta [\epsilon^\eta (1 - 2n_g^\eta) \sigma_z^\eta + \Delta^\eta \sigma_x^\eta] + \lambda \sigma_z^a \sigma_z^b, \quad (6)$$

where  $\epsilon^{a(b)} = 2e^2(C_t^{b(a)} + C_c)/\Lambda$  with  $\Lambda = C_t^a C_t^b - C_c^2$ ,  $\Delta^\eta = E_J^\eta$ ,  $\lambda = e^2 C_c / \Lambda$ ,  $\eta \in \{a, b\}$  and  $\sigma_{x,z}$  denotes the corresponding Pauli matrix in the basis of  $\{|0\rangle, |1\rangle\}$ . The single-device terms in Hamiltonian (6) can be tuned to be zero by conventional methods [17]. Therefore, in what follows, we do not take them into consideration. For two identical devices ( $C_0^\eta = C_0$ ),  $\epsilon = 4E_c$  and  $\lambda = e^2 C_c / (C_t^2 - C_c^2) \simeq 2\beta E_c$  with  $\beta = C_c / C_0$ . It is notable that the strength of this interaction, proportional to the coupling capacitance, is stronger than any other present-known coupling methods.

The circuit Hamiltonian of the two coupled chains, as depicted in Fig. 2, can be obtained in a similar way. In this extended multipartite coupling case, the long-range interaction between the devices would appear, which decays exponentially as  $\beta^{|i-j|}$  with  $i$  and  $j$  being the site labels of the two involved devices [18]. Therefore, the long-range interaction is negligible if  $\beta \ll 1$ , and in typical experiments  $\beta \simeq 0.05$  [19]. Up to the first order of  $\beta$ , the interaction Hamiltonian is given by

$$H_{JJ} = \sum_{\eta;j} \lambda_{\eta} \sigma_{z;j}^{\eta} \sigma_{z;(j+1)}^{\eta} + \sum_j \lambda_c \sigma_{z;j}^a \sigma_{z;j}^b, \quad (7)$$

where  $\lambda_{\eta} \simeq e^2 C_{\eta} / [C_0 + 2(C_c + 2C_{\eta})]$  and  $\lambda_c \simeq e^2 C_c / [C_0 + 2(C_c + C_a + C_b)]$ .

Once the coupled chains are placed according to the geometry of Fig. 1(a), a corresponding two-dimensional square lattice model is constructed. Drawing an analogy between the device states in chain  $a$  ( $b$ ) and spin  $\uparrow$  ( $\downarrow$ ), the above interaction Hamiltonian in the addressed system may be rewritten as the two-component fermion model of Eq. (1), with the parameters  $(\lambda_a, \lambda_b, \lambda_c)$  corresponding to  $(J_q, J_p, U)$  [20]. As a result, the topologically protected ground state of Eq. (4) may be implemented with the present setup of superconducting devices.

In addition, to accomplish certain topological quantum manipulation tasks, including the examination of the anyon statistics, it is a must to have a set of basic operations of the devices. In the Majorana fermion representation, the wanted operations are [13]

$$S_{j_b}^z = i\chi_{j_b} \psi_{j_b}, \quad S_{j_w}^z = i\chi_{j_w} \psi_{j_w}, \quad (8a)$$

$$S_{j_b}^x = \psi_{j_b} \prod_{j < j_b} (i\chi_j \psi_j), \quad S_{j_w}^x = \chi_{j_w} \prod_{j < j_w} (i\chi_j \psi_j), \quad (8b)$$

where  $S_j^z$  is the spin-flip operator for a given site and it also transfers a double fermion occupancy to empty or vice versa.  $S_j^x$  denotes a nonlocal operation that creates or annihilates a fermion at site  $j$  and changes the site occupation for sites  $j < j_{b(w)}$  [13]. In the present model,  $S^z$  and  $S^x$  are effective Pauli matrices, which, according to Ref. [4], may create and move the excitations.

At this stage, let us elaborate how to obtain the wanted operations in Eqs. (8a) and (8b). Notably, individual addressability is normally a prerequisite in such manipulation. In the present proposal, the size of the device setup is macroscopic, thus individual addressability is taken as granted. To manipulate the states, we put the lattice into a microwave cavity, with the geometry of the hybrid system being explained in the caption of Fig. 3. For simplicity, we consider only the single-mode standing wave cavity. To be more specific, we reach the cavity assisted manipulation by a magnetic drive [21]. The interaction can be switched on/off by modulating the external magnetic field to be ac/dc [21]. With the dc magnetic flux, the external flux is merely used to address separately the single-qubit rotations. Under the cavity field, it is also readily possible to tune off single-qubit terms. The wanted operations in

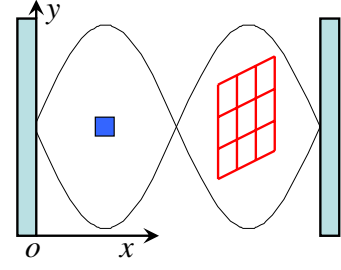


FIG. 3: (Color online) A schematic diagram of the cavity-assisted manipulation. The  $x$  and  $y$  coordinates are denoted by the arrows, and the  $z$  direction is pointing out the  $xy$  plane. The square lattice (red) is placed to be parallel to the  $yz$  plane. The square lattice and the auxiliary device (blue rectangle) are placed with the  $x$  coordinate at the antinodes of the single-mode standing-wave cavity. All superconducting devices are placed with their loop plane being parallel to the  $xoz$  plane, which is perpendicular to the magnetic component of the cavity field, letting it be the only contributed component.

Eq. (8a) for selected device can be achieved with the cavity mediated integrations by tuning the driven magnetic flux of the device to be of ac. The Pauli matrices  $S_{j_w}^z$  and  $S_{j_b}^z$  in Eq. (8a) correspond to  $\sigma_x \otimes \sigma_x$  and  $\sigma_y \otimes \sigma_y$  two-body interaction of two devices of  $j$ th site, respectively. These two type interactions for each lattice site can be directly engineered in our hybrid implementation [21] as it allows selected addressing of designated devices. These two interactions are mediated by the virtue cavity photon, thus we need to keep the cavity mode in the vacuum state. Here, the devices work in their degeneracy points.

The common cavity mode can also be used to realize the global stringlike  $S^x$  operators in Eq. (8b). The off-resonant interaction between the cavity mode and the selected devices is [22]

$$H_{QND} = \chi n_c \sum_j \sigma_j^z, \quad (9)$$

where  $n_c = a^\dagger a$  is the photon number operator of the cavity mode, the coupling strength is  $\chi = g^2/2\delta$  with  $g$  as the single-photon Rabi frequency for the cavity mode, and  $\delta$  is the detuning between the cavity mode frequency  $\omega_c$  and optical transition frequency in atomic spins. In our implementation, this can be the  $|1\rangle \rightarrow |2\rangle$  transition of the selected devices, where  $|2\rangle$  is an ancillary energy level beyond the qubit subspace  $\{|0\rangle, |1\rangle\}$ , and the frequency of the drive ac flux satisfies  $\omega = \tilde{\omega}_{12} + \omega_c + \delta$  with  $\tilde{\omega}_{12} = 2E_c(3 - 2n_g)/\hbar$ . To avoid the transitions  $|0\rangle \rightarrow |1\rangle$  and  $|0\rangle \rightarrow |2\rangle$  by the ac drive, we tune  $\tilde{\omega}_{01} = 2E_c(1 - 2n_g)/\hbar$  via  $n_g$  so that  $\delta \ll \Delta_{1,2}$ , where  $\Delta_1 = \omega - \tilde{\omega}_{01}$  and  $\Delta_2 = \tilde{\omega}_{01} + \tilde{\omega}_{12} - \omega$  are the corresponding detunings. This quantum non-demolition (QND) Hamiltonian (9) preserves the photon number of the cavity mode. Within the  $n_c \in \{0, 1\}$  subspace, the evolution of the QND Hamiltonian during the interaction time  $\tau = \pi/2\chi$  yields [10]

$$U = \exp[-iH\tau] = \begin{cases} \mathbf{I} & \text{for } n_c = 0 \\ (-i)^N \prod_j \sigma_j^z & \text{for } n_c = 1 \end{cases} \quad (10)$$

where  $N$  is the number of the selected devices. From Eq. (10), (controlled) string operations for an arbitrary string can be achieved [10].

If the cavity is initially prepared in the  $n_c = 1$  state, the global operation reduces to the string operation  $U_z = \prod_j \sigma_j^z$ . As all string operators are equivalent to  $U_z$  up to local single spin rotations [10], all string operations for arbitrary string can be achieved:  $U_x = \prod_j \sigma_j^x = H U_z H$  and  $U_y = \prod_j \sigma_j^y = R U_z R$ , where  $H = \prod_j H_j$  and  $R = \prod_j R_j$  with  $H_j = (\sigma_j^x + \sigma_j^z) / \sqrt{2}$  being the Hadamard rotation and  $R_j = \exp(-i\frac{\pi}{4}\sigma_j^z)$ . Therefore, with this elementary operation, creation and manipulation of anyons are likely feasible in our scheme. For example,

$$\begin{aligned} S_{j_b}^x &= \psi_{j_b} \prod_{k_b < j_b} (i\chi_{k_b} \psi_{k_b}) \prod_{k_w < j_b} (i\chi_{k_w} \psi_{k_w}) \\ &= \sigma_{y;j}^b \prod_{k_b < j_b} (i\sigma_{x;k_b}^a \sigma_{x;k_b}^b) \prod_{k_w < j_b} (i\sigma_{y;k_w}^a \sigma_{y;k_w}^b), \end{aligned} \quad (11)$$

denotes a nonlocal operation that could create a domain-wall-like excitation/semion (at the site  $j$ ) from the ground states under the open boundary condition [13].

If the cavity is initially prepared in a superposition of zero- and one-photon states, the global operation in Eq. (10) reduces to a controlled-string operation:  $U_{cs} = \mu|0\rangle\langle 0| \otimes I + \nu|1\rangle\langle 1| \otimes U_z$ , where the parameters  $\mu$  and  $\nu$  are controlled by the initially prepared photon number state. With such a controlled-string operation, one is able to access the topological memory and to build anyonic interferometry [10].

In simulating the string operations, we need to engineer the cavity number states. Therefore, beside the square lattice, we also place an ancilla device in the cavity, as shown in Fig. 3, which is used to control the cavity photon number state by swapping its states with that of the cavity using the resonate cavity-device interaction. This swap operation can be achieved by the famous Jaynes-Cummings model Hamiltonian:  $H_{JC} = \Omega (a\sigma^+ + a^\dagger\sigma^-)$ , which can be implemented in our system by choosing the frequency of the ac driven magnetic flux for the ancillary device satisfying  $\omega = \omega_c + \tilde{\omega}_{01}$ . In this case, we need to tune the device slightly away from the degeneracy point, which results in a shorter decoherence time. Fortunately, the resonate operation is also much faster.

In summary, we have proposed an exotic scheme to implement a two-component fermion model using superconducting quantum circuits, which was shown to support abelian anyonic excitations. Most intriguingly, we have elaborated how to achieve all the wanted operations that could create and manipulate the anyonic states. Our approach provides an experimentally feasible scenario to access the topological memory and to build the anyonic interferometry.

We thank Yue Yu, L. B. Shao and Liang Jiang for many helpful discussions. This work was supported by the RGC of Hong Kong under Grants No. HKU7045/05P and No. HKU7049/07P, the URC fund of HKU, the NSFC under Grants No. 10429401, No. 10674049 and No. 10625416, and the National Basic Research Program of China (No. 2006CB921800, No. 2007CB925204 and No. 2009CB929300).

- 
- [1] X.-G. Wen, *Quantum Field Theory of Many-Body Systems* (Oxford University Press, New York, 2004).
- [2] C. Nayak, S. H. Simon, A. Stern, M. Freedman, and S. Das Sarma, *Rev. Mod. Phys.* **80**, 1083 (2008).
- [3] A. Kitaev, *Ann. Phys. (N.Y.)* **303**, 2 (2003).
- [4] A. Kitaev, *Ann. Phys. (N.Y.)* **321**, 2 (2006).
- [5] Y.-J. Han, R. Raussendorf, and L.-M. Duan, *Phys. Rev. Lett.* **98**, 150404 (2007).
- [6] L.-M. Duan, E. Demler, and M. D. Lukin, *Phys. Rev. Lett.* **91**, 090402 (2003).
- [7] A. Micheli, G. K. Brennen, and P. Zoller, *Nat. Phys.* **2**, 341 (2006).
- [8] J. Q. You, X.-F. Shi, and F. Nori, e-print arXiv:0809.0051.
- [9] C. Zhang, V. W. Scarola, S. Tewari, and S. Das Sarma, *Proc. Natl. Acad. Sci. U.S.A.* **104**, 18415 (2007).
- [10] L. Jiang, G. K. Brennen, A. V. Gorshkov, K. Hammerer, M. Hafezi, E. Demler, M. D. Lukin, and P. Zoller, *Nat. Phys.* **4**, 482 (2008).
- [11] M. Aguado, G. K. Brennen, F. Verstraete, and J. I. Cirac, *Phys. Rev. Lett.* **101**, 260501 (2008).
- [12] S. Dusuel, K. P. Schmidt, and J. Vidal, *Phys. Rev. Lett.* **100**, 177204 (2008).
- [13] Y. Yu and Y. Li, e-print arXiv:0806.1688.
- [14] X.-Y. Feng, G.-M. Zhang, and T. Xiang, *Phys. Rev. Lett.* **98**, 087204 (2007); H.-D. Chen and Z. Nussinov, *J. Phys. A: Math. Theor.* **41**, 075001 (2008).
- [15] Although it is hard to figure out the presence of anyons directly from Hamiltonian (1), it is quite clear from the theory of Kitaev [4] that Hamiltonian (3) does support anyonic excitations from the ground state denoted by Eq. (4).
- [16] J. Q. You, X. Hu, and F. Nori, *Phys. Rev. B* **72**, 144529 (2005).
- [17] J. Q. You and F. Nori, *Phys. Today* **58** (11), 42 (2005); Y. Makhlin, G. Schön, and A. Shnirman, *Rev. Mod. Phys.* **73**, 357 (2001).
- [18] G. P. Berman, A. R. Bishop, D. I. Kamenev, and A. Trombettoni, *Phys. Rev. B* **71**, 014523 (2005).
- [19] Y. Nakamura, Yu. A. Pashkin, and J. S. Tsai, *Phys. Rev. Lett.* **87**, 246601 (2001); Yu. A. Pashkin, T. Yamamoto, O. Astaffev, Y. Nakamura, D. V. Averin, and J. S. Tsai, *Nature (London)* **421**, 823 (2003).
- [20] It is noted that the signs before  $\lambda_a$  and  $\lambda_b$  in Hamiltonian (7) are initially positive. However, the signs can be tuned to be minus by a proper redefinition of the analogy between device states  $\{|0\rangle, |1\rangle\}$  and pseudospin states  $\{|+\rangle, |-\rangle\}$ , i.e.,  $|0\rangle$  ( $|1\rangle$ ) corresponds to  $|+\rangle$  ( $|-\rangle$ ) for all odd-number sites while  $|0\rangle$  ( $|1\rangle$ ) corresponds to  $|-\rangle$  ( $|+\rangle$ ) for all even-number sites.
- [21] S.-L. Zhu, Z. D. Wang, and P. Zanardi, *Phys. Rev. Lett.* **94**, 100502 (2005); Z.-Y. Xue, Z. D. Wang, and S.-L. Zhu, *Phys. Rev. A* **77**, 024301 (2008); e-print arXiv:0806.0753.
- [22] M. O. Scully, and M. S. Zubairy, *Quantum optics* (Cambridge University Press, New York, 1997).